

Characterization of Pressure Signals in a Bubble Column by Wavelet Packet Transform

Soung Hee Park[†] and Sang Done Kim*

Department of Chemical Engineering, Woosuk University, Chonbuk 565-701, Korea

*Department of Chemical Engineering, Korea Advanced Institute of Science and Technology, Daejeon 305-701, Korea

(Received 3 May 2002 • accepted 20 November 2002)

Abstract—All experiments of pressure fluctuations were carried out in a bubble column with a moderately large column of 0.376 m ID. The recently developed technique of wavelet packet transform based on localized wavelet functions is applicable to analysis of the fluctuating signals. The time series of pressure fluctuation signals have been analyzed by means of wavelet packet transform components, decomposition through best basis algorithm and time-frequency representation. By resorting to this technique, the objects in bubbly flow regime have fine scales and frequencies than ones in churn-turbulent flow regime. Thus, this wavelet packet transform method enables us to obtain the frequency content of local complex flow behaviors in a bubble column.

Key words: Bubble Column, Pressure Fluctuation, Wavelet Packet Transform, Best Basis Algorithm, Flow Regime

INTRODUCTION

Bubble columns have been widely adopted for various chemical, pharmaceutical and biochemical systems as reactors, contactors and separation units since they have exhibited high heat and mass transfer rates due to efficient contact between the phases during continuous operation [Park, 1989; Shah et al., 1982; Shumpe and Deckwer, 1987]. Judicious design and effective operation of a bubble column demand a thorough understanding of the hydrodynamic properties of the reactors. Towards this end, numerous investigators have extensively studied pressure fluctuations [Harry and Akker, 1998; Kang et al., 1998; Kwon et al., 1994; Park, 1989; Park et al., 2001].

The Fourier transform and its inverse establish a one-to-one relation between the time domain and the frequency domain, which is a widely used classical analysis tool. This transform uses the sine and cosine as its bases to map a time domain function into frequency domain. Thus, the spectrum shows the global strength with which any frequency is contained in the function. However, the Fourier transform does not show how the frequencies vary with time in the spectrum. Nevertheless, time-varying frequencies are quite common in natural phenomena, e.g., seismic signals and non-stationary geophysical process [Kumar and Georgiou, 1994]. To investigate such phenomena, we need a transform that enables us to obtain the frequency content of a process locally in time.

The wavelet packet transform and wavelet transform has attracted growing attention from mathematicians as well as engineers [Park and Kim, 2001; Park et al., 2001], because it uses linear combinations of wavelet functions to represent signals. The following are some characteristics that make the wavelet approximations remarkable and useful: wavelets are localized in time and are good building block functions for a variety of signals, including signals with

features which change over time and signals which have jumps and other non-smooth features. A traditional Fourier series approximation is not well suited to these types of signals. Wavelet packet components separate a signal into multiresolution components. The fine and coarse resolution components capture the fine and coarse scale features in the signal, respectively.

We applied both Fourier transform and wavelet packet transform to pressure fluctuation signals in a bubble column and then compared the two techniques. We proposed the wavelet packet transform as a new alternative tool for identification of bed properties in bubble column reactor.

THEORETICAL

Wavelet packet analysis is an important generalization of wavelet analysis [Coifman and Wickerhauser, 1992; Wickerhauser, 1994]. Wavelet packet functions comprise a rich family of building block functions. Although still localized in time, wavelet packet functions offer more flexibility than wavelets in representing different types of signals. In particular, wavelet packets are better at representing signals that exhibit oscillatory or periodic behavior. Wavelet packet functions are generated by scaling and translating a family of basic function shapes, which include father wavelets $\phi(t)$ and mother wavelets $\psi(t)$. In addition to $\phi(t)$ and $\psi(t)$, there is a whole range of wavelet packet functions $W_b(t)$. These functions are parameterized by an oscillation or frequency index b . A father wavelet corresponds to $b=0$, $\phi(t) \equiv W_0(t)$. A mother wavelet corresponds to $b=1$, $\psi(t) \equiv W_1(t)$. Larger values of b correspond to wavelet packets with more oscillations and higher frequency.

Wavelet packet approximations are based on translated and scaled wavelet packet functions $W_{j,b,k}(t)$. These are generated from the base functions W_b as follows:

$$W_{j,b,k}(t) = 2^{-j/2} W_b(2^{-j}t - k) \quad (1)$$

The wavelet packet $W_{j,b,k}$ has scale 2^j and location $2^j k$, where j , b , and k are resolution level index, oscillation index, and time index, respectively. As in wavelet analysis, the index j corresponds to the

[†]To whom correspondence should be addressed.

E-mail: drpark@woosuk.ac.kr

*This paper is dedicated to Professor Dong Sup Doh on the occasion of his retirement from Korea University.

resolution level and the index k corresponds to the translation shift. However, for a wavelet packet, there is also the oscillation parameter b .

In wavelet packet analysis, a signal $f(t)$ is represented as a sum of orthogonal wavelet packet functions $W_{j,b,k}(t)$ at different oscillations, scales, and locations:

$$f(t) \approx \sum_j \sum_b \sum_k W_{j,b,k} W_{j,b,k}(t). \quad (2)$$

The range of the summation for the levels j and the oscillations b is chosen so that the wavelet packet functions are orthogonal.

Wavelet packet analysis starts with construction of a wavelet packet table. Like the discrete wavelet transform (DWT), a wavelet packet table has coefficients at different resolution levels and translations. However, a wavelet packet table also has coefficients corresponding to different oscillations. At resolution level j , the table has wavelet packet coefficients with oscillation indices $b=0, 1, \dots, 2^j-1$. By contrast, for each resolution level, the DWT has coefficients at just one oscillation index (or two at the resolution level).

Suppose we have n sampled signal values $f=(f_1, f_2, \dots, f_n)$ where n is a multiple of 2^J . The wavelet packet table has $J+1$ resolution levels where J is the maximum resolution level. At resolution level j , a table has n coefficients, divided into 2^j coefficient blocks or crystals. When we stack the $J+1$ resolution levels on top of one another, we get the $(J+1) \times n$ table of coefficients, divided by 2^{J+1} blocks. A crystal is a set of coefficients arranged on a lattice. A wavelet packet crystal $w_{j,b}$ is indexed by level j and oscillation b :

$$w_{j,b} = (w_{j,b,1}, w_{j,b,2}, \dots, w_{j,b,n/2^j}). \quad (3)$$

Coifman and Wickerhauser [1992] developed the "best basis" al-

gorithm for selecting optimal bases from wavelet packet tables. The best basis algorithm automatically adapts the transform to best match the characteristics of the signal.

EXPERIMENTS

The bubble column apparatus, which is shown in Fig. 1, is composed of a column, a perforated plate and a bottom section. All experiments were carried out in a Plexiglas column at room temperature under atmospheric pressure. The column's inside diameter was 0.376 m, and its height was 2.1 m. A perforated plate served as the liquid distributor. The fluidizing liquid ($U_l=0-0.10$ m/s) and gas ($U_g=0.02-0.10$ m/s) were water and oil-free compressed air, respectively. The pressure tap for measuring pressure fluctuations was located at 0.4 m above the distributor. The differential pressure transducer generated output voltages proportional to the pressure fluctuation signals. The signals were stored in a data acquisition system (Data Precision Model, D-6000) and processed by a personal computer.

Once a steady state was reached, the fluctuating voltage-time signals, corresponding to the fluctuating pressure-time signals, from the differential pressure transducer were sampled at a rate of 0.01 s and stored in the data acquisition system. The overall data acquisition time was 41 s, thereby yielding a total of 4100 data points. The signals were transmitted to the computer. Wavelet packet transform of the pressure fluctuation using the S+Wavelet software (MathSoft Inc.) was calculated from the digitized data acquired. We used

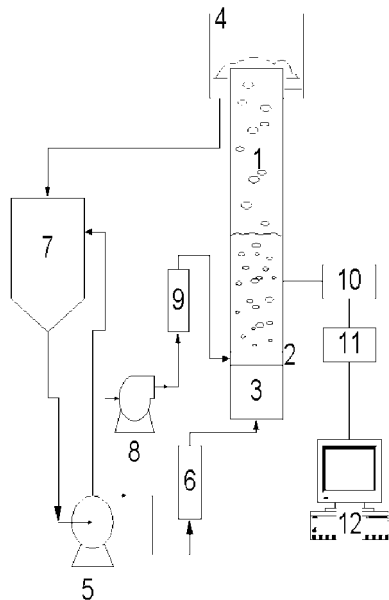


Fig. 1. Schematic diagram of experimental apparatus.

- | | |
|--------------------|-----------------------------|
| 1. Main column | 7. Liquid reservoir |
| 2. Distributor | 8. Air compressor |
| 3. Calming section | 9. Gas flowmeter |
| 4. Weir | 10. Pressure transducer |
| 5. Pump | 11. Data acquisition system |
| 6. Flowmeter | 12. PC |

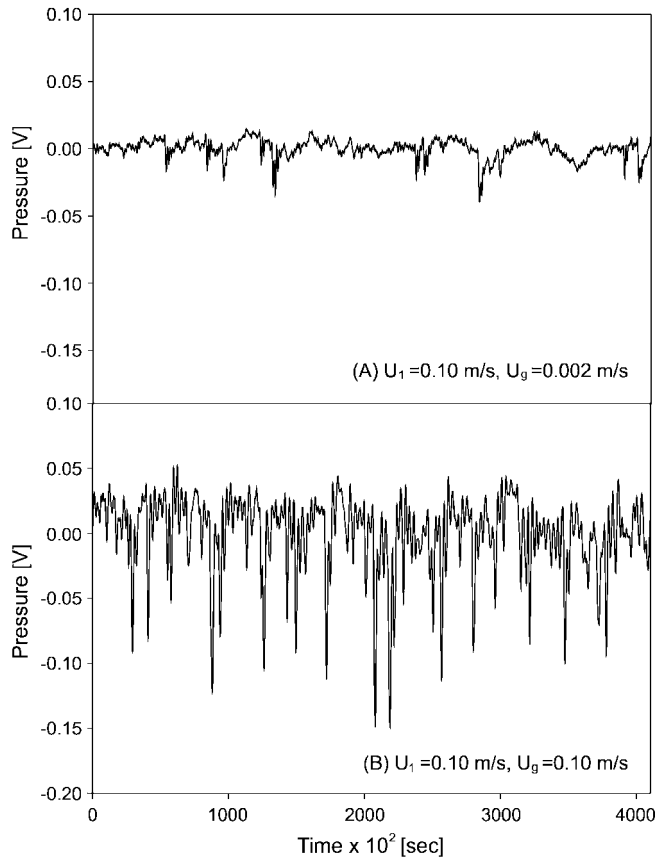


Fig. 2. Pressure fluctuation signals in (A) a bubbly flow regime and (B) a churn-turbulent flow regime in a bubble column.

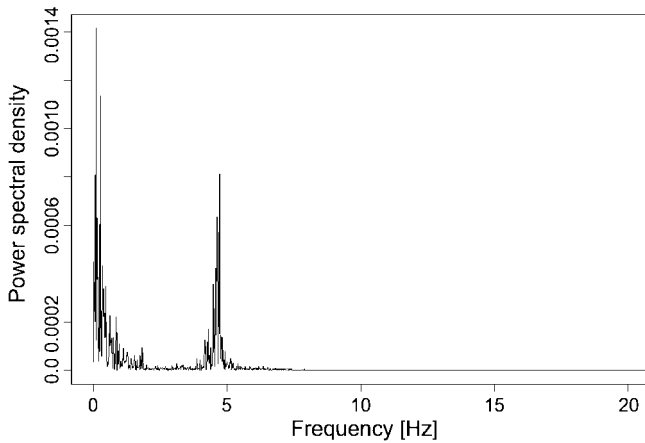


Fig. 3. Typical power spectral density of a signal in a bubbly flow regime ($U_l=0.10$ m/s, $U_g=0.02$ m/s).

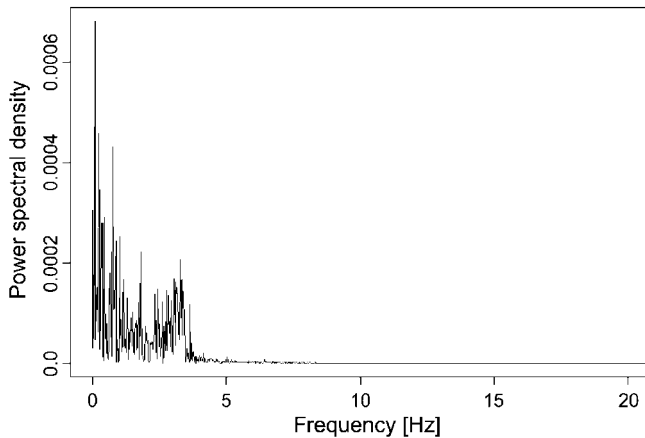


Fig. 4. Typical power spectral density of a signal in a churn-turbulent flow regime ($U_l=0.02$ m/s, $U_g=0.10$ m/s).

Coifman wavelet as mother wavelet.

RESULT AND DISCUSSION

The typical power spectral density functions of pressure fluctuations from bubbly flow regime and churn-turbulent flow regime (see Fig. 2), respectively, were calculated and presented in Figs. 3 and 4. A peak or peaks in the spectrum correspond to a major periodic component or components in the random variable [Park, 1989; Lee and Kim, 1988]. Note that in Figs. 3 and 4, distinct peaks appear between 0 and 10 Hz in the power spectral density function. These peaks indicate the existence of corresponding objects of the frequencies, usually, bubbles. The Fourier transform yields the energy density in an individual frequency averaged over a whole time. As can be seen in power spectrums, the Fourier basis function is localized only in the frequency but not in time. Even though the power spectral density functions indicate that the major frequency is generated by bubbles, it cannot reveal the movement of those bubbles over time. This is a disadvantage of the Fourier transform, which is unable to permit time localization.

Figs. 5 and 6 show plots of a wavelet packet table of wavelet packet transform for a pressure fluctuation at different flow regimes. And

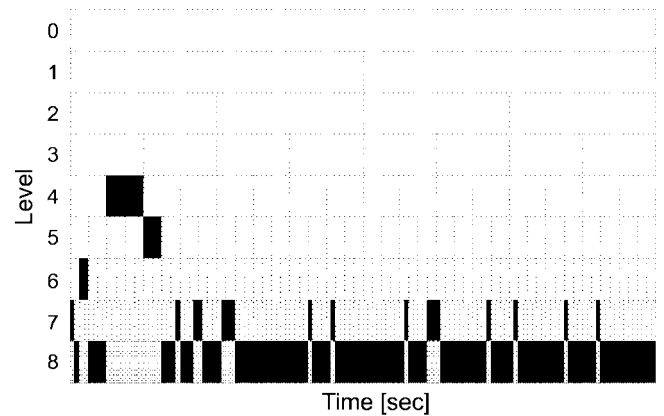


Fig. 5. Wavelet packet table of a signal in a bubbly flow regime ($U_l=0.10$ m/s, $U_g=0.02$ m/s).

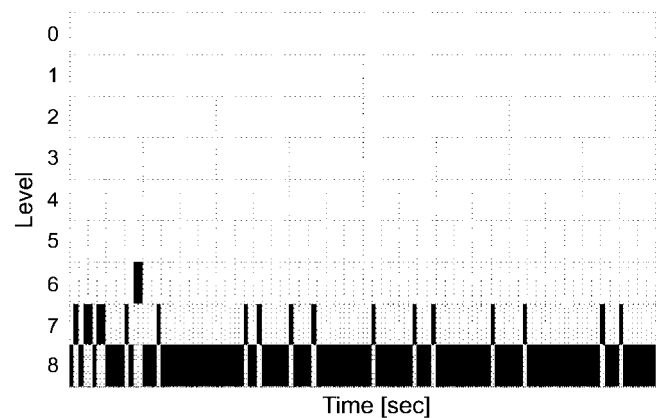


Fig. 6. Wavelet packet table of a signal in a churn-turbulent flow regime ($U_l=0.02$ m/s, $U_g=0.10$ m/s).

the best basis from a wavelet packet table was computed and selected by using the Coifman and Wickerhauser best basis algorithm [Coifman and Wickerhauser, 1992]. The best bases were composed of different crystals, which are shaded in black. As in the plots, each wavelet packet coefficient occupies a box having a constant area. The height of the box depends on the scale of the wavelet packet: fine scale coefficients occupy tall thin boxes and coarse scale coefficients occupy flat wide boxes. As can be seen in Fig. 5, the computed and selected bases of the pressure fluctuation signal in the bubbly flow regime were composed of crystals such as $W_{7,0}$, $W_{8,1}$, $W_{6,1}$, $W_{4,1}$, $W_{5,4}$, etc., which were located at coarse scales and fine scales. The high frequency oscillations are captured by the fine scale bases, e.g., $W_{4,1}$, $W_{5,4}$, and the coarse scale bases, e.g., $W_{7,0}$, $W_{8,1}$, correspond to lower frequency oscillations. And the bases for the churn-turbulent flow regime (see Fig. 6) were composed of the coarse scale ones such as $W_{7,1}$, $W_{8,0}$, $W_{7,7}$, $W_{7,6}$, $W_{8,1}$, etc. It indicates that the pressure fluctuation signal obtained was decomposed by these bases with the coarse scales and fine scales.

The plots of wavelet packet components are shown in Figs. 7 and 8. The signal components are ordered by energy, with the highest energy components plotted at the top. According to wavelet packet decomposition, a signal is reconstructed by a sum of wavelet packet components. A signal in a bubbly flow regime ($U_l=0.10$ m/s, $U_g=$

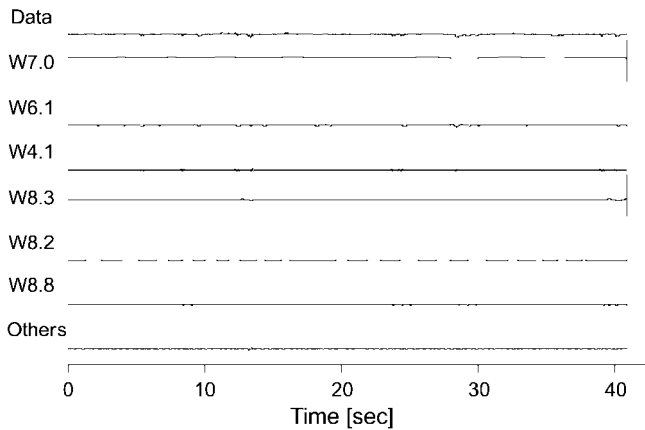


Fig. 7. Plot of wavelet packet components of a signal in a bubbly flow regime ($U_i=0.10$ m/s, $U_g=0.02$ m/s).

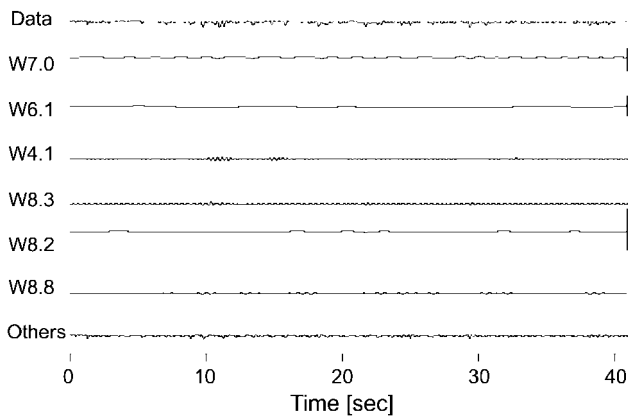


Fig. 8. Plot of wavelet packet components of a signal in a churn-turbulent flow regime ($U_i=0.02$ m/s, $U_g=0.10$ m/s).

0.02 m/s) is represented as a sum of wavelet packet components such as $W_{7,0}$, $W_{8,1}$, $W_{6,1}$, $W_{4,1}$, $W_{5,4}$, and others (Fig. 7), while a signal in a churn-turbulent flow regime ($U_i=0.02$ m/s, $U_g=0.10$ m/s) is made by a sum of components such as $W_{7,1}$, $W_{8,0}$, $W_{7,7}$, $W_{7,6}$, $W_{8,1}$, and others (Fig. 8). The high frequency oscillations are captured mainly by the fine scale components, e.g., $W_{6,1}$, $W_{5,4}$, $W_{4,1}$. The coarse scale components, $W_{8,6}$, correspond to lower frequency oscillations. As can be seen in these figures, the highest energy components in the bubbly flow regime are finer than the ones in the churn-turbulent flow regime. It is well known that the bubble size and population increase and the bubble interactions become significant with increasing gas velocity (churn-turbulent flow regime). Also, from the change of the pattern over the time in these plots of wavelet packet decomposition of the pressure fluctuations, we can estimate the passage of the bubbles in the bed.

Time-frequency analysis is concerned with how the frequency representation of the signal changes over time. Using a wavelet packet transform, we can construct a time-frequency plot by dividing the time-frequency plane into rectangles. The modulus of each wavelet packet coefficient determines the gray level of each rectangle. The spectrogram produces an easily interpretable visual two-dimensional representation of signals. As can be seen in Figs. 9 and 10, spectrograms of the pressure signals are obtained at different flow

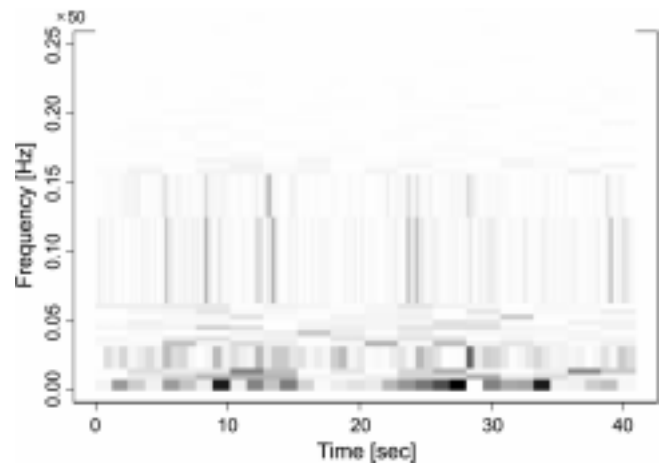


Fig. 9. Spectrogram of a signal in a bubbly flow regime ($U_i=0.10$ m/s, $U_g=0.02$ m/s).

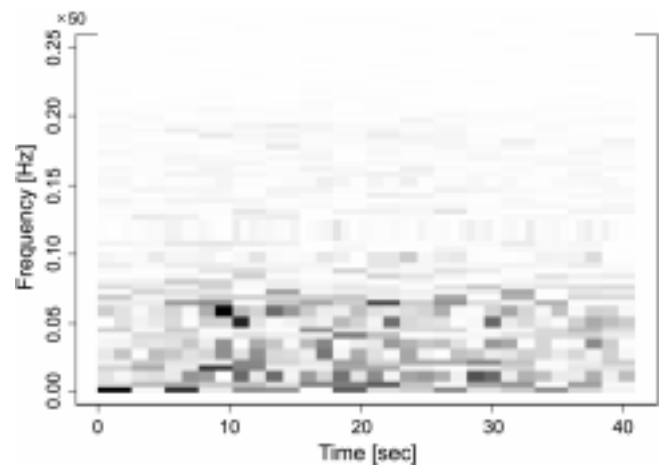


Fig. 10. Spectrogram of a signal in a churn-turbulent flow regime ($U_i=0.02$ m/s, $U_g=0.10$ m/s).

regimes, bubbly flow regime ($U_i=0.10$ m/s, $U_g=0.02$ m/s) and churn-turbulent flow regime ($U_i=0.02$ m/s, $U_g=0.10$ m/s), respectively. The level of energy of an individual time-frequency cell is indicated as a shade of gray: The darker the cell, the higher the energy content of the time-frequency cell. In the churn-turbulent flow regime the cells corresponding to low frequency are more shaded and energetic. The bigger the bubble size, the greater the energy content of cells in the lower frequency ranges. This is consistent with the result from evaluation of the power spectrum by Fourier transform. Also, these figures show that the cells change over time at each frequency. It means that the spectrogram obtained by wavelet packet transform using best basis algorithm provides both the localization of frequency and time, and makes it possible to identify and classify the status of the bed.

CONCLUSIONS

The differential pressure fluctuation has been analyzed by resorting to the wavelet packet transform analysis and Fourier transform. The time series of pressure fluctuations have been analyzed by means of discrete wavelet packet transform components and spectrogram.

According to the analysis by wavelet packet table and spectrogram, the objects in the bubbly flow regime have finer scales and frequencies than ones in churn-turbulent flow regime. These are useful tools to identify the flow regime of the bubble column. Consequently, the wavelet packet transform is expected to be useful for analyzing the pressure fluctuation signals to understand the hydrodynamics in a bubble column.

ACKNOWLEDGMENT

This research was supported by Woosuk University.

NOMENCLATURE

DWT: discrete wavelet transition
 F : frequency [Hz]
 J : maximum resolution level
 t : time [sec]
 U_g : gas velocity [m/s]
 U_l : liquid velocity [m/s]
 W : wavelet packet function

Greek Letters

Ψ : wavelets, mother wavelet
 ϕ : scaling function

Subscripts

b : oscillation or frequency index
 j : resolution level index
 k : time index

REFERENCES

- Coifman, R. and Wickerhauser, V., "Entropy-Based Algorithms for Best Basis Selection," *IEEE Transactions on Information Theory*, **38**, 713 (1992).
- Harry, E. A. and Akker, V. D., "Coherent Structures in Multiphase Flows," *Powder Technology*, **100**, 123 (1998).
- Kang, Y. M., Ko, H., Park, S. H., Fan, L. T. and Kim, S. D., "Mixing of Particles in Gas-Liquid-Solid Fluidized Beds Containing a Binary Mixture of Particles," *I&EC Research*, **37**, 4167 (1998).
- Kang, Y., Cho, Y. J., Woo, K. J., Kim, K. I. and Kim, S. D., "Bubble Properties and Pressure Fluctuations in Pressurized Bubble Columns," *Chem. Eng. Sci.*, **55**, 411 (2000).
- Kang, Y., Cho, Y. J., Woo, K. J. and Kim, S. D., "Diagnosis of Bubble Distribution and Mass Transfer in Pressurized Bubble Columns with Viscous Liquid Medicine," *Chem. Eng. Sci.*, **54**, 4887 (1999).
- Kumar, P. and Foufoula-Georgiou, E., "Wavelets in Geophysics," Academic Press, Australia (1994).
- Kwon, H. W., Han, J. H., Kang, Y. and Kim, S. D., "Bubble Properties and Pressure Fluctuations in Bubble Columns," *Korean J. Chem. Eng.*, **11**, 204 (1994).
- Lee, G. S. and Kim, S. D., "Pressure Fluctuations in Turbulent Fluidized Beds," *J. Chem. Eng. Japan*, **21**, 515 (1988).
- Park, S. H., "Phase Holdups and Pressure Fluctuations in Two- and Three-Phase Fluidized Beds," Master Thesis, Korea Advanced Institute of Science and Technology (1989).
- Park, S. H., Kang, Y., Cho, Y. J., Fan, L. T. and Kim, S. D., "Characterization of Pressure Signals in a Bubble Column by Wavelet Transform," *J. of Chem. Eng. of Japan*, **34**, 158 (2001).
- Park, S. H. and Kim, S. D., "Wavelet Transform Analysis of Pressure Fluctuation Signals in a Three-Phase Fluidized Bed," *Korean J. Chem. Eng.*, **18**, 1015 (2001).
- Shah, Y. T., Kelkar, B. G., Godbole, S. P. and Deckwer, W. D., "Design Parameters Estimations for Bubble Column Reactors," *AIChE J.*, **28**, 353 (1982).
- Shumpe, A. and Deckwer, W. D., "Viscous Media in Tower Bioreactors: Hydrodynamic Characteristics and Mass Transfer Properties," *Bioprocess Eng.*, **2**, 79 (1987).
- Wickerhauser, V., "Adapted Wavelet Analysis-from to Theory to Software," A. K. Peters, Ltd. (1994).